Available online at www.sciencedirect.com
SCIENCE DIRECT®
Journal of Nuclear Materials 337–339 (2005) 99–103
journal of nuclear materials
www.elsevier.com/locate/jnucmat

Outer divertor target deposited layers during reversed magnetic field operation in JET

P. Andrew [a,*], J.P. Coad [a], Y. Corre [b], T. Eich [c], A. Herrmann [c], G.F. Matthews [a], J.I. Paley [d], L. Pickworth [a], R.A. Pitts [e], M.F. Stamp [a], JET EFDA Contributors [1]

[a] *Euratom/UKAEA Fusion Association, Culham Science Centre, Abingdon, Oxon OX14 3DB, UK*
[b] *Association Euratom-VR, KTH-Physic Department, 106 91 Stockholm, Sweden*
[c] *Association EURATOM, Max-Planck-Institut fur Plasmaphysik, D-85748 Garching, Germany*
[d] *Plasma Physics Group, Blackett Laboratory, Prince Consort Road, London SW7 2AZ, UK*
[e] *CRPP Association EURATOM-Confederation Suisse, EPFL, CH-1015 Lausanne, Switzerland*

Abstract

Divertor surface temperatures are significantly affected by the presence of deposited surface layers. This phenomenon can be used to monitor deposited layer evolution on a shot-by-shot basis. It was found that during an experimental campaign where the $\mathbf{B} \times \nabla B$ direction was reversed that the outer target, normally an erosion zone, became a deposition zone.

PACS: 61.80.B; 81.15; 52.40.H; 52.55.F
Keywords: Erosion and deposition; Divertor asymmetry; JET; Thermography

1. Introduction

In general, material eroded from the first wall of a fusion reactor will not be redeposited locally. The resultant areas of net erosion and deposition affect component lifetime and tritium retention, respectively. The normal pattern of material migration seen in the JET post-mortem analysis is deposition at the inner divertor target and slight erosion over the outer. The deposited material is primarily carbon [1]. Although the various experimental observation give a consistent picture, the physics behind this long-range material migration pattern is not well understood.

In this paper we show that infrared thermography can be used to map out the zones of net deposition. The signature of this deposition is an anomalously high thermal resistance on the surfaces under observation [2]. The areas of thermal resistance correspond to areas of deposited layers. This permits a study of the shot to shot dependence of deposition over a reasonably wide region not possible with post-mortem analysis nor with any other technique currently in use on a large tokamak.

2. Results

In JET plasmas with steady conditions (e.g. no ELMs), it is possible to get an accurate measure of the

* Corresponding author.
E-mail address: pla@jet.uk (P. Andrew).
[1] See annex of J. Pamela et al., Fusion Energy 2002 (Proc. 19th Int. Conf. Lyon, 2002), IAEA, Vienna.

0022-3115/$ - see front matter © 2004 Published by Elsevier B.V.
doi:10.1016/j.jnucmat.2004.10.145

total power to the divertor target, P_{div}, from the input power to the plasma, P_{in} and the radiated power, P_{rad}.

$$P_{\mathrm{div}} = P_{\mathrm{in}} - (1-g) \times P_{\mathrm{rad}}, \quad (1)$$

where g is the fraction of the radiated power which is incident on the divertor, typically 15%. This relation is supported by thermocouples imbedded in the JET divertor tiles which measure the total energy content of the divertor for each pulse [3]. Furthermore, the thermocouples can be used to determine the power sharing between the two legs of the divertor. The power asymmetry has been found to depend on the direction of $\mathbf{B} \times \nabla B$ and on the heating power [4].

While excess surface temperature due to impurities affects the determination of the power to the target by infrared, the area of power deposition remains clear. Using the power to the target calculated from Eq. (1), and the power asymmetry $A \equiv P_{\mathrm{outer\,div}}/P_{\mathrm{inner\,div}}$ together with the wetted area, it is possible to calculate the power density to the inner and outer targets separately. Knowing the bulk thermal properties or the tiles, the temperature rise at the divertor tiles in the absence of any surface layer can then be calculated. Comparison of this temperature with the actual measured temperature will indicate the presence or absence of a surface layer.

Fig. 1 shows such a comparison for a deuterium plasma with neutral beam injection (NBI) heating. The plasma changes from a limiter to divertor configuration at 13 s, and at 15 s the strike points move up to the vertical target plates, this being the best position for infrared (IR) viewing, and back to the horizontal target plates at 28 s. Fig. 1(a) shows the plasma heating power (ohmic + NBI), which has been increased in discrete steps, but stays below the L–H mode transition threshold. Also shown are the total radiated power, which is about 30% of the input power in this case, and the resulting $P_{\mathrm{inner\,div}}$ using equation Eq. (1), and the fact that $A \sim 3$ for this pulse. Fig. 1(b) shows the peak target temperature at the inner vertical target plate as described above. Also shown are the peak temperature actually measured by a 2d IR camera [2], and the temperature measured by a thermocouple 10 mm below the surface. Fig. 1(c) is a plot of the difference between measured and calculated peak surface temperatures in Fig. 1(b) normalized by $P_{\mathrm{inner\,div}}$ from Fig. 1(a). Note that there is good agreement between calculated and measured surface temperatures only after the power is switched off. The excess temperature at the inner target is ~100–150 K/(MW/m^2) of incident power, and dominates the observed temperature. Within the uncertainty of the above calculation (the relative effect of radiation on $P_{\mathrm{outer\,div}}$ and $P_{\mathrm{inner\,div}}$, the uncertainty in the power dependence of the power asymmetry and the wetted area) the excess temperature is directly proportional to incident power.

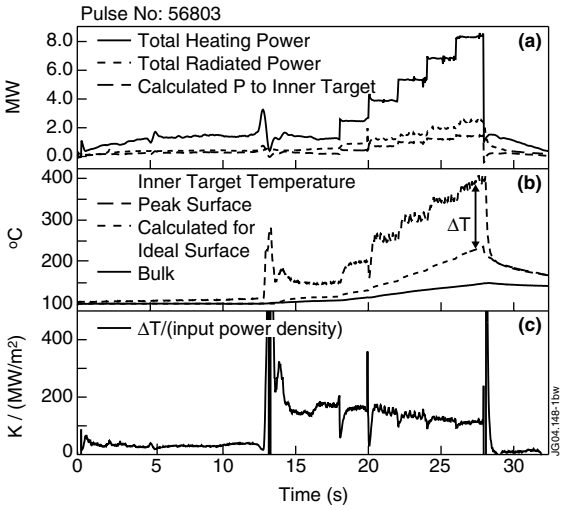

Fig. 1. Inner target, deuterium pulse, forward field: (a) plasma heating, and radiated powers, together with power conducted to inner target, (b) measured and calculated inner target temperature, (c) inner target surface temperature rise, nomalized to conducted power to inner target.

Fig. 2 shows the excess surface temperature (per unit power density) for the inner and outer targets for the 3 years of JET operation. The calculation has been limited to plasmas with a similar divertor configuration, all either ohmic or L-mode. While there is an enormous amount of scatter, there are several clear trends. First, with the exception of the period near the reversed B campaign, the excess temperature is consistently much larger on the inner target. Second, if the excess temperature is associated with impurity deposition, one might expect a linear increase with time as the deposit grew thicker. However over the range shown, which represents two thirds of the target's life to date, there is no such trend. This saturation phenomenon is seen again for the outer target data: during the reversed B campaign. The excess surface temperature persisted at a level comparable to that observed for the outer target, about ~150 K/(MW/m^2), for ~300 pulses, while it only took 100 pulses to rise to that level. The effect of a helium campaign on the excess surface temperature is described in [2].

3. Discussion

3.1. Thermal model for the surface layer

The apparent saturation of the excess surface temperature suggests that the thermal resistance is not due to low thermal conductivity of the deposited material. Another possibility is that the thermal resistance results from poor thermal contact between the deposited layer

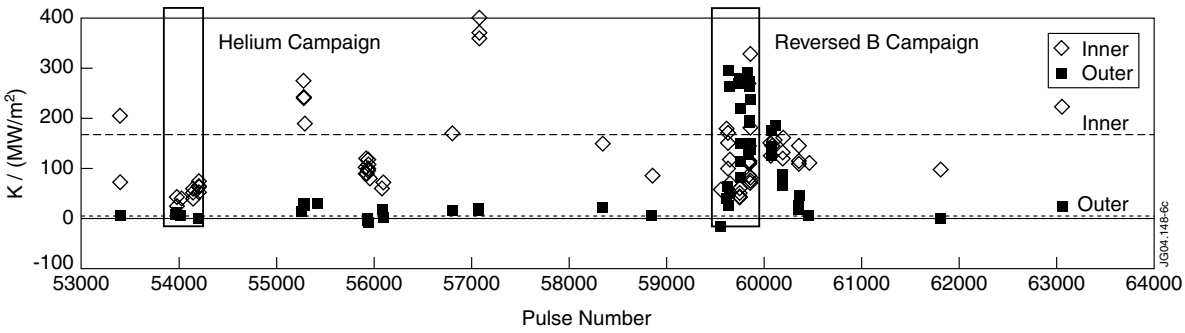

Fig. 2. Excess temperature per input power for inner and outer targets over a period of 3 years operation. Dashed lines indicated the average value excluding operation in reversed B or He.

and the substrate. The two situations are indistinguishable for the case of the steady heating situations analyzed above, but can profoundly affect the interpretation of transient heat fluxes such as ELMs.

One method to determine heat fluxes from the surface temperature is to assume that there is an excess temperature at the surface proportional to the incident power [5]:

$$T_{\text{surface}} - T_{\text{bulk}} = q/\alpha, \tag{2a}$$

where q is the incident power density, and T_{bulk} is the temperature just below the surface. For no surface layer, $\alpha \to \infty$ and $T_{\text{bulk}} \to T_{\text{surface}}$. In this description, $1/\alpha$ is precisely the quantity plotted in Fig. 1(c), and Fig. 2. The average values correspond to $\alpha_{\text{inner}} = 6\ \text{kW/m}^2\text{/K}$, and $\alpha_{\text{outer}} = 200\ \text{kW/m}^2\text{/K}$. In Fig. 1, it does indeed appear that α is a constant.

Extending the above model to a case of a layer with poor thermal contact with the underlying surface gives instead of Eq. (2a),

$$T_{\text{surface}} - T_{\text{bulk}} = q_{\text{back}}/\alpha, \tag{2b}$$

$$q_{\text{front}} - q_{\text{back}} = C_0\,\mathrm{d}T_{\text{surface}}/\mathrm{d}t, \tag{3}$$

where q_{front}, q_{back} are the heat flux densities into the front and out the back of the surface layer, and C_0 the thermal mass of the layer. The characteristic cooling time for a heat pulse is $\tau = C_0/\alpha$. For the case where the characteristic time of the heating is much longer than τ, Eqs. (2b) and (3) reduce to Eq. (2a). For the case where the characteristic heating is much shorter than τ, the temperature response for a heat pulse of amplitude q_0 and duration Δt is

$$0 < t < t_0, \quad \Delta T_{\text{surface}} = q_0 t/C_0, \tag{4a}$$

$$t > t_0, \quad \Delta T_{\text{surface}} = (q_0/\alpha)(\Delta t/\tau)\exp(-t/\tau). \tag{4b}$$

If the model with no thermal mass (Eq. (2a)) is applied to the above temperature evolution, the resultant power is

$$0 < t < t_0, \quad q = q_0 t/\tau, \tag{5a}$$

$$t > t_0, \quad q = q_0(\Delta t/\tau)\exp(-t/\tau) \tag{5b}$$

i.e. the peak heat flux density is smaller by a factor $\Delta t/\tau$, the duration is longer by a factor $\tau/\Delta t$, but the total energy density, $\int q\,\mathrm{d}t$, is unchanged. This means that even if the model with no thermal mass is applied to a situation where that is a poor assumption, the ELM energies deduced will still be accurate.

3.2. Application to an ELM

Fig. 3 shows the peak temperature evolution at the inner strike point during a pair of ELMs. The temperature rises in ~0.5 ms, but decays over a much longer

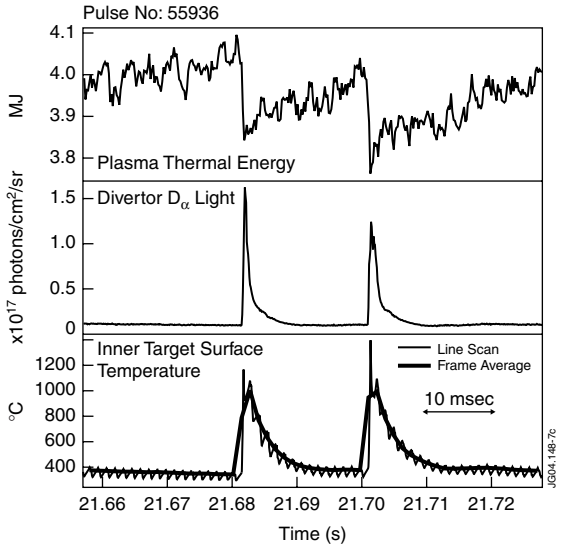

Fig. 3. The temperature evolution at the inner target for ELMy H-mode plasma (55936). The jitter with ~1.3 ms period is an artefact of the IR measurement which scans an image line by line at a rate 1.3 ms/frame.

timescale, ~5 ms. In 5 ms other diagnostic signatures of ELMs, magnetic perturbations and D_α light, have long since died away, so it is hard to believe that there is still ELM energy flowing onto the target over such a long time. Instead this is believed to be due to a long cool down as described Eq. (4b).

If Eq. (4b) is applied to the temperature cool down in Fig. 3, using $\alpha_{inner} = 6\ kW/m^2/K$ from Fig. 2, then the thermal capacity of the inner target, $C_0 = \tau\alpha_{inner}$, is $30\ J/m^2/K$. Assuming that the heat capacity of the deposited layer is the same as the underlying target, the implied thickness of the layer is ~10 μm. In reality, the deposited layer is probably not as dense as the substrate. This thickness is approximately 5× lower than the thickness of deposits measured by surface analysis [1].

3.3. Asymmetric impurity accumulation

In normal JET operation there is a clear asymmetry in the impurity deposition on the divertor: the outer divertor experiences slight net erosion, while the inner divertor is a zone of net deposition [1]. The amount of material deposited in the divertor is more than the divertor erosion, implying that the main chamber walls are also a source of impurities deposited in the divertor [6,7]. The net erosion at the outer divertor is consistent with the disappearance of the surface layer seen the by IR after returning to forward field operation.

During reversed field operation, however, impurities were being deposited on the outer divertor as implied by the infrared observation of the surface layer growth. During this same period other changes in the normal behavior of the inner and outer legs of the divertor were observed. The inner divertor plasma density and temperatures became similar to the outer divertor [8]. The outer divertor became the dominant contribution to the exhausting of neutrals [9]. Deposition of impurities on a quartz microbalance in the inner divertor pump slot was reduced, sometimes going negative (erosion) [10].

What remains unclear is whether the $\mathbf{B} \times \nabla B$ direction has affected the source of impurities incident on inner and outer targets, or whether the change in relative divertor plasma density and temperature upsets the balance between erosion and deposition at each leg. In forward field the inner divertor plasma can have very high density and low temperature, conditions favourable to net deposition.

The fact that the outer divertor conditions change very little in reverse field is the strongest evidence to support the argument that the deposition asymmetry is due to a source asymmetry. If there is a net flow of impurities to the outer divertor in reverse field, which is absent in forward field, it would be consistent with the measured flows in the SOL [11]. In forward field a large flow in the scrap off layer is measured at the top of the vessel, towards the inner divertor. In reverse field this is a stagnation point. Taken together, these 2 measurements suggest than there is an impurity source at the low field side of the tokamak. These results do not rule out an impurity source on the high field side as well. Finally, an independent indication that the SOL flows drag impurities is the result that tracer ^{13}C injected at the top of the plasma in forward field could only be found at the inner divertor [12].

4. Conclusions

The anomalously high surface temperature at the JET inner divertor can be described by a deposited layer having poor thermal contact with the substrate. This is supported by the slow cool down observed on the inner target after ELMs. During experiments with the direction of $\mathbf{B} \times \nabla B$ reversed, a thermally resistant layer was observed to grow on the *outer* target plates. Given that the outer divertor plasma density and temperature do not depend on the field direction, it is concluded that there was a net source of impurities flowing to the outer target. Gradual disappearance of the layer upon returning to forward field confirms that the outer target is a net erosion zone under these conditions. The implied impurity flow in the plasma boundary is consistent with the measured SOL flow, provided there is an impurity source at the low field side of the tokamak.

Acknowledgments

This work has been conducted under the European Fusion Development Agreement and is partly funded by Euratom and the United Kingdom Engineering and Physical Sciences Research Council.

References

[1] J.P. Coad et al., J. Nucl. Mater. 313–316 (2003) 419.
[2] P. Andrew et al., J. Nucl. Mater. 313–316 (2003) 135.
[3] G.F. Matthews et al., J. Nucl. Mater. 290–293 (2001) 668.
[4] Y. Corre, in: Proceedings of the 31st EPS Conference on Controlled Fusion and Plasma Physics, 2004.
[5] A. Herrmann, ASDEX Upgrade Team, Europhysics Conference, Abstracts (CD-ROM, Proceedings of the 28th EPS Conference on Controlled Fusion and Plasma Physics, Madeira 2001), 2001, p. 2109.
[6] G.F. Matthews et al., Proceedings of the 30th EPS Conference on Controlled Fusion and Plasma Physics, 2003, P-3.198.
[7] M.F. Stamp, 10th International Workshop on Carbon Materials for Fusion Application, 17–19 September 2003, Juelich, Germany.
[8] A. Huber et al., these Proceedings, doi:10.1016/j.jnucmat.2004.10.123.

[9] M. Lehnen et al., in: Proceedings of the 31st EPS Conference on Controlled Fusion and Plasma Physics, 2004.
[10] G. Esser et al., these Proceedings, doi:10.1016/j.jnucmat.2004.10.112.
[11] R.A. Pitts et al., these Proceedings, doi:10.1016/j.jnucmat.2004.10.111.
[12] J. Likonen et al., J. Fus. Eng. Des. 66–68 (2003) 219.